Research on Engineering Structures & Materials

journal homepage: http://www.jresm.org

Research Group

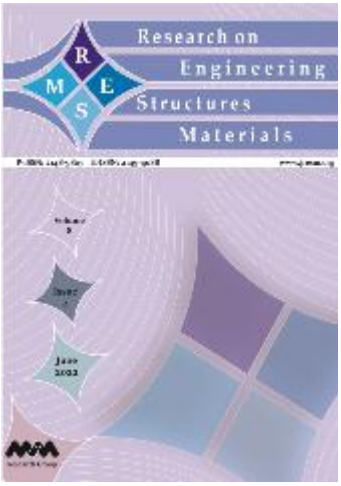

Numerical investigation of the combined effects of coating layer properties and specific heat capacities of materials on the heat transfer mechanism in solidification of pure metals

Mehmet Hakan Demir

Online Publication Date: 5 Sep 2022

URL: http://www.jresm.org/archive/resm2022.441me0602.html
DOI: http://dx.doi.org/10.17515/resm2022.441me0602

Journal Abbreviation: *Res. Eng. Struct. Mater.*

To cite this article
Demir MH. Numerical investigation of the combined effects of coating layer properties and specific heat capacities of materials on the heat transfer mechanism in solidification of pure metals. *Res. Eng. Struct. Mater.*, 2022; 8(4): 751-772.

Disclaimer
All the opinions and statements expressed in the papers are on the responsibility of author(s) and are not to be regarded as those of the journal of Research on Engineering Structures and Materials (RESM) organization or related parties. The publishers make no warranty, explicit or implied, or make any representation with respect to the contents of any article will be complete or accurate or up to date. The accuracy of any instructions, equations, or other information should be independently verified. The publisher and related parties shall not be liable for any loss, actions, claims, proceedings, demand or costs or damages whatsoever or howsoever caused arising directly or indirectly in connection with use of the information given in the journal or related means.

Published articles are freely available to users under the terms of Creative Commons Attribution - NonCommercial 4.0 International Public License, as currently displayed at here (the "CC BY - NC").

Research on Engineering Structures & Materials
journal homepage: http://www.jresm.org
MIM Research Group

Research Article

Numerical investigation of the combined effects of coating layer properties and specific heat capacities of materials on the heat transfer mechanism in solidification of pure metals

Mehmet Hakan Demir

Department of Mechatronics Engineering, Iskenderun Technical University, Hatay, Turkey
Department of Mechanical and Industrial Engineering, University of Illinois at Chicago, Chicago, IL, USA

Article Info

Article history:
Received 02 Jun 2022
Revised 01 Aug 2022
Accepted 30 Aug 2022

Keywords:

Solidification;
Pure metal;
Casting;
Phase-change;
Heat transfer;
Finite difference;
Growth instability

Abstract

Mold coating has a critical importance to adjust the microstructure of the cast and regulate the heat transfer during the solidification. The phase change heat transfer problem during the solidification is solved numerically in the presence of the coating layer and finite thermal capacitances of materials. Previous studies have been expanded by considering the combined effects of the coating layer and specific heat capacities of the materials on growth instability. Also, the conditions are specified based on the process parameters for minimizing or eliminating the unstable growth of the shell. The complexness of the two-dimensional thermal problem is reduced by perturbation analysis. After that, the governing equations are solved numerically by using the variable time step and grid size based Lagrangian finite difference scheme. The effects of the thermal properties of the materials, coating properties and the thermal contact resistances on the thermoelastic instability process are studied in detail. According to the results obtained that a thicker coating layer causes more regular growing and better quality in the shell. However, the specific heats of the solidified layer and coating materials have stabilizing effects but an increase in the mold specific heat leads to a destabilizing effect on the thermoelastic instability. Also, the thermal conductivities have great impact on growth of the shell. The solution of this study can be used as thermal part in uncoupled and coupled problems in which the thermomechanical problems are investigated.

© 2022 MIM Research Group. All rights reserved.

1. Introduction

Almost all metals and alloys, some ceramic and polymer materials are liquid at some stage of their production and start to solidify when they are cooled below the melting temperature. The control of thermo-mechanical events that occur during casting is of great importance to increase the quality of the casting. Studies, in which the solidification during casting is analyzed theoretically and experimentally, reveal that thermo-mechanical phenomena at the solid/liquid interface (moving interface) has significant effect on the thermoelastic unstable growth that occurs during solidification. When the experimental studies are examined, it is seen that some undulations occur at the moving interface during the solidification of metals as an inevitable result of cooling [1]. The experiments reveal that these undulations continue from the beginning of solidification to a certain stage and then disappear. This behavior is explained as the thermal and mechanical phenomena occurring at the mold/shell interface affects the thermo-mechanical conditions at the moving interface and this situation gradually disappears with the increase of the solidified shell thickness. These non-uniform undulations occur because of the uneven heat flux at the mold/shell interface. This unstable undulation causes important faults such as

Corresponding author: mhakan.demir@iste.edu.tr
orcid.org/0000-0002-3934-2425
DOI: http://dx.doi.org/10.17515/resm2022.441me0602

micro/macro scaled cracks in the final casting [3]. This phenomenon during the solidification, which is called thermoelastic instability, is theoretically examined in two parts such as thermal and mechanical problems. The thermal problem and its solution are discussed in this study in detail.

The phase-change problems (moving interface problems) have great importance for the applications such as purification of metals, casting/welding processes and thermal energy storage systems [4]. The common property of phase change problems is a moving interface that occurs between the solid and liquid phases during the solidification or melting process and the location of this moving interface have to be determined with the solution. Stefan [5] dealt with the first theoretical work on solving the phase-change problem for the ice formation process. Evans [6] and Douglas [7] studied the existence and uniqueness of this problem's solution, respectively. Since then, despite many phase change problems appeared in literature but exact solution to this problem has been limited to idealized cases containing semi-finite or infinite regions with simple boundary and initial conditions. The history and some classical solutions to the Stefan problems were collected in Crank [8] and Hill [9]. Due to the nonlinear behavior of this problem, the superposition principle is not applicable and all cases are evaluated separately.

Barry and Caunce [10] solved Stefan type problem numerically and analytically by taking into the account of linear and nonlinear diffusivities. Song et al. [11] solved the Stefan problem by an underlying iso-geometric approximation with a sharp interface. For the solution of one-dimensional Stefan problems with moving boundaries, Reutskiy [12] developed a delta-shaped function based meshless numerical. Juric and Tryggvason [13] used the front tracking method and the fixed grid in space was used for determining the moving boundary's location and the interface heat sources were calculated by using the moving grid on the interface. An adapted grid procedure is applied by Murray and Landis [14] and they found that the moving interface location is determined more accurately with the adapted grid method. Also, an adaptive grid method is used by Segal et al. [15] for the free boundary in the 2D phase change problem and the movement of the grid was introduced into the system equations by use of Arbitrarian Lagrangian-Eulerian (ALE) approach. Kutluay et al. [16] obtained a solution of Stefan problem by using boundary immobilization techniques with variable space grid. Caldwell et al. [17] solved 1D Stefan problem by using the nodal integral method with finite difference (FD) scheme. The methods for the numerical solution of one-dimensional Stefan problems for different geometries are compared in Caldwell and Kwan [18] in detail. A simple level set method was used to solve the Stefan problem in the dendritic solidification process by Chen et al. [19]. Font [20] solved the one-phase phase-change problem with size-dependent thermal conductivity. The boundary immobilization and finite difference scheme are used for numerical solution. Moreover, the phase-field modeled Stefan problems are investigated by Mackenzie and Robertson [21] and Sun and Beckermann [22]. Vynnycky and Mitchell [23] developed an algorithm for 1D time-dependent problem by use of the Keller box FD scheme and boundary immobilization technique. Myers and Mitchell [24] developed a solution method for solving Stefan problem based on the heat balance integral method that is called the combined integral method. This method breaks down like other integral methods when the boundary temperature approaches zero or oscillates.

The problem of solidification of metals with phase-change heat transfer has been specifically addressed in this paper and some studies about heat transfer during solidification are summarized below. Zabaras and Mukherjee [25] solved the phase change problem during the pure metal solidification process by convolution integrals and Green's functions based boundary element method. In Dursunkaya and Nair [26], the motion of a solidification front is analyzed by using a semi-analytical approach during the solidification of a finite one-dimensional medium with boundary temperature with oscillations.

Skrzypczak and Wergrzyn-Skrzypczak [27] studied the mathematical and numerical modeling of the heat transfer problem during the pure metal solidification process by using the finite element method and the front tracking method based on the level set method were used for determining the position of the moving interface. Another useful method for analyzing Stefan problems is the perturbation method. Caldwell and Kwan [28] solved Stefan problems, which have time-dependent boundary conditions, by using perturbation method. Yu et al. [29] obtained a perturbation solution to the planar solidification problem with time-dependent heat generation. Yigit [30] used the linear perturbation method for solving a 2D phase-change Stefan problem during the solidification process in which the planar mold's outer surface has a periodic temperature boundary condition. Also, Yigit [31] used the same method to determine the heat transfer problem's solution during pure metal solidification on a mold with sinusoidal surfaces, and the governing equations were discretized by using the finite difference approach. A linear perturbation solution was used to obtain approximate analytical and numerical solutions of the 2D heat conduction problem for solidification on a planar mold surface by Yigit [32] and the effects of thermal diffusivity of shell on the unstable growth were determined. The previous paper was extended by taking into account the thermal diffusivity of the mold in Yigit [33] and the linear perturbation and the finite difference methods are used for the solution.

As it is mentioned above, the uneven shell growth leads to defects in the cast product because of the uneven heat transfer during the solidification. Mold coating is the one of the most used and effective techniques to control the heat transfer. It plays an effective role in ensuring controlled solidification by reducing the solidification rate of the liquid metal in the mold. Thus, the liquid proceeds without freezing in the metal mold and fills the entire mold. On the other hand, the mold coatings are used to prevent direct contact with the liquid metal with the mold steel and to increase the life of the mold by preventing corrosive effects and soldering. Another advantage of using mold coating is that it assists with casting release from the mold [34]. In the literature, there are many experimental studies in which the coating's effects are investigated in detail. However, the number of theoretical studies are much less than the experimental ones. Jafari et al. [35] studied experimentally on the mold coating effects on the thin-wall ductile iron casting. The effects of coating thickness on porosity percentage and imperfection during the casting process of Al-Si-Cu alloy are studied experimentally by Karimian et al. [36]. Also, the effects of mold coating properties and alloy composition on the heat transfer during the casting of Al alloys are determined by Hamasaiid et al. [37]. Demir and Yigit solved the heat transfer problem for the pure metal solidification on a coated planar mold in [4,38-40] for coupled and uncoupled processes by neglecting the effects of thermal diffusivities. The same problem is modeled for a sinusoidal mold and coating in Demir and Yigit [41] and the linear perturbation method was used to solve it analytically.

In this study, the numerical solution of the heat transfer problem for the early stages of the full solidification problem, in which the pure metal solidification occurs on the coated planar mold, is made by considering the finite thermal diffusivity of the materials. The previous studies are extended by investigating the combined effects of the properties of the coating layer and thermal diffusivities of the materials. The problem is modeled with the linear perturbation method for reducing the complexness of the problem and then, it is discretized by the variable time and grid size based Lagrangian finite difference scheme for numerical solution. After that, the effects of the coating properties are investigated theoretically and the key question is that how can be adjusted the coating layer's properties depending on the other process parameters. Also, other system parameters associated with the presence of the coating layer such as thermal contact resistances, specific heats of the layers, and thermal conductivity ratios between the materials are investigated in detail. This problem has extended the dissertation work given in [4] by adding the heat capacities of the materials and the solution obtained as a result of this

problem will be used in the realization of the thermo-mechanic solution, in which the thermal problem affects the mechanical problem.

This paper is organized as follows. The two-dimensional modeling and the perturbation analysis for simplifying the problem by reducing dimensionality are described in Sections 2 and 3, respectively. Section 3 introduces the terminology used throughout this paper. In Section 4, dimensionless variables are introduced which are used to simplify the complexness of the problem and generalize the solution. Section 5 shows the numerical algorithm used to solve the problem and Section 6 includes the results and their discussions which indicate the reliability of the proposed numerical algorithm and the effects of the system parameters. The conclusions of the study are given in Section 7.

2. Mathematical Formulation

The geometry of the considered solidification process is shown in Fig. 1. The coating, shell and mold layers are denoted with superscripts b, c and d respectively.

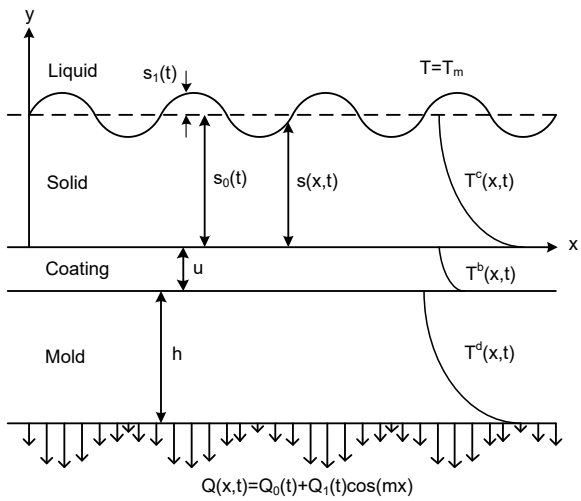

Fig. 1 Geometry of the casting process

There is a moving surface between the liquid/solid phases of shell material and it has a sharp structure. The reason for this is that the phase change during the pure metal solidification process occurs at a distinct temperature. The materials' properties don't change depending on the time and temperature. The temperature fields in these solid layers ($T^i(x,y,t), i = c,b,d$) and instantaneous location of the freezing front ($s(x,t)$) are determined as a result of the solution. The liquid shell's temperature is assumed to be at the melting temperature T_m during the process. For this reason, the thermal effects of the liquid phase of the metal are not taken into account. This assumption provides us that the moving interface's temperature is always equal to T_m.

Since the thermal diffusivities of the materials are taken into account in this study, the solution is obtained numerically due to the non-linearity. In this numerical solution, a limiting solution to the problem is used for initial conditions. The limiting solution is obtained analytically [38] by assuming the thermal diffusivities of the materials are infinite. This makes the thermal capacitance of the solid layers are zero and the general heat conduction equations are solved analytically with boundary and initial conditions. The solution procedure is explained in Appendix and Ref. [38].

In Figure 1, h and u symbolize thicknesses of the mold and its coating, respectively. As it is mentioned that the thermal diffusivities are assumed to be finite and therefore, the distribution of thermal fields in the solid layers varies parabolically. The temperature fields have to satisfy the equations in Eq. (1).

$$\begin{aligned}
\frac{\partial^2 T^c}{\partial y^2}(x,y,t) &= \frac{1}{\alpha^c}\frac{\partial T^c}{\partial t}(x,y,t) \\
\frac{\partial^2 T^b}{\partial y^2}(x,y,t) &= \frac{1}{\alpha^b}\frac{\partial T^b}{\partial t}(x,y,t) \\
\frac{\partial^2 T^d}{\partial y^2}(x,y,t) &= \frac{1}{\alpha^d}\frac{\partial T^c}{\partial t}(x,y,t)
\end{aligned} \tag{1}$$

where α^i $(i = b, c, d)$ denotes the thermal diffusivities of the materials. These equations are solved depending on the boundary conditions. The moving interface's temperature, which is equal to T_m is defined in Eq. (2).

$$T^c(x,s,t) = T_m \tag{2}$$

The energy balance at the moving interface due to heat conduction and the latent heat is;

$$K^c \frac{\partial T^c}{\partial y}(x,s,t) = L^c \rho^c \frac{ds}{dt}(x,t) \tag{3}$$

where L^c and ρ^cdenote latent heat and density of the shell, respectively. K^i, ($i = c, b, d$) represents the thermal conductivities of the materials. Eqs. (4) and (5) show the heat flux continuity at the interfaces between the solid layers, respectively.

$$K^c \frac{\partial T^c}{\partial y}(x,0,t) = K^b \frac{\partial T^b}{\partial y}(x,0,t) \tag{4}$$

$$K^b \frac{\partial T^b}{\partial y}(x,-u,t) = K^d \frac{\partial T^d}{\partial y}(x,-u,t) \tag{5}$$

In the model, there are thermal contact resistances at the interface between the solid layers due to contaminant films and roughness. R_{sc} and R_{cm} symbolize these constant thermal resistances at the interfaces. The subscript "sc" denotes the shell-coating interface and subscript "cm" indicates the coating-mold interface. These contact resistances are assumed to be independent of the contact pressure. This is true for the uncoupled process in which the thermal problem affects the mechanical problem but vice versa does not come true. The uncoupled model is applicable for the early stages of the process and this means that the solution of this full solidification problem is eligible for very early stages. Eq. (6) define this relation between heat flux and thermal contact resistances.

$$\begin{aligned}
K^c \frac{\partial T^c}{\partial y}(x,0,t) &= \frac{1}{R_{sc}}[T^c(x,0,t) - T^b(x,0,t)] \\
K^b \frac{\partial T^b}{\partial y}(x,-u,t) &= \frac{1}{R_{cm}}[T^b(x,-u,t) - T^d(x,-u,t)]
\end{aligned} \tag{6}$$

At the mold's lower surface, there is a heat flux, $Q(x,t)$, and it has small spatial variation to perform the uneven heat transfer. The heat flux extracted from the mold is given in Eq. (7).

$$K^d \frac{\partial T^d}{\partial y}(x, -u-h, t) = Q(x,t) \tag{7}$$

3. Perturbation Analysis

The conditions at the interfaces between the solid layer control the resulting properties of the final cast and the solidification rate. In this method, it is assumed that an x-dependent perturbation grows on the unperturbed process. The parameters of the unperturbed process affect the development of this perturbation. The unperturbed and perturbed processes are called as zeroth-order and first-order processes, respectively. The amplitudes of the perturbed quantities are very smaller than the zeroth-order quantities and the perturbation is linear. So, this provides us to use Fourier transformation in x and the dimensionality and complexness of the problem are reduced.

The new forms of the heat flux, the temperature fields, and the moving interface's position are

$$Q(x,t) = Q_0(t) + Q_1(t)cos(mx) \tag{8}$$

$$T(x,y,t) = T_0(y,t) + T_1(y,t)cos(mx) \tag{9}$$

$$s(x,t) = s_0(t) + s_1(t)cos(mx) \tag{10}$$

Subscript 0 and 1 define the zeroth-order process and the first-order process, respectively. The constant m and λ denote the wavenumber and the wavelength and they depend each other with $\lambda = 2\pi/m$. Also, the slope of the moving front, $\partial s/\partial x$, is very much less than unity. If the readers need more information about the perturbation method, they refer to Yigit's paper in Refs. [32] and [33].

Accordingly, the perturbation added forms of temperature field in Eq. (9) substitutes into Eq. (1), and then the periodic and uniform terms are separated. The obtained uniform (zeroth-order) terms from heat conduction equations are;

$$\begin{aligned} \frac{\partial^2 T_0^c}{\partial y^2}(y,t) &= \frac{1}{\alpha^c}\frac{\partial T_0^c}{\partial t}(y,t) \\ \frac{\partial^2 T_b^c}{\partial y^2}(y,t) &= \frac{1}{\alpha^b}\frac{\partial T_b^c}{\partial t}(y,t) \\ \frac{\partial^2 T_0^d}{\partial y^2}(y,t) &= \frac{1}{\alpha^d}\frac{\partial T_0^d}{\partial t}(y,t) \end{aligned} \tag{11}$$

The obtained periodic (first-order) terms from separating heat conduction equations are;

$$\begin{aligned} \frac{\partial^2 T_1^c}{\partial y^2}(y,t) - m^2 T_1^c(y,t) &= \frac{1}{\alpha^c}\frac{\partial T_1^c}{\partial t}(y,t) \\ \frac{\partial^2 T_1^b}{\partial y^2}(y,t) - m^2 T_1^b(y,t) &= \frac{1}{\alpha^c}\frac{\partial T_1^b}{\partial t}(y,t) \\ \frac{\partial^2 T_1^d}{\partial y^2}(y,t) - m^2 T_1^d(y,t) &= \frac{1}{\alpha^c}\frac{\partial T_1^d}{\partial t}(y,t) \end{aligned} \tag{12}$$

Temperature fields are expanded in form of Taylor series at the vicinity of $y = s_0(t)$. The boundary conditions are rearranged similarly to heat equations and the second and higher-order terms are eliminated due to their negligible effects. The zeroth and first order boundary conditions to be used in the solution of the equations in Eqs. (11) and (12) are determined by using perturbed forms in Eqs (8)-(10). The procedure is described in detail in Ref [33]. See this reference for details.

The zeroth-order boundary conditions are;

$$T_0^c(s_0,t) = T_m \tag{13}$$

$$K^c \frac{\partial T_0^c}{\partial y}(s_0,t) = L_c \rho_c \frac{ds_0}{dt}(x,t) \tag{14}$$

$$K^c \frac{\partial T_0^c}{\partial y}(0,t) = K^b \frac{\partial T_0^b}{\partial y}(0,t) \tag{15}$$

$$K^b \frac{\partial T_0^b}{\partial y}(-u,t) = K^d \frac{\partial T_0^d}{\partial y}(-u,t) \tag{16}$$

$$K^c \frac{\partial T_0^c}{\partial y}(0,t) = \frac{1}{R_{sc}}[T_0^c(0,t) - T_0^b(0,t)] \tag{17}$$

$$K^b \frac{\partial T_0^b}{\partial y}(-u,t) = \frac{1}{R_{cm}}[T_0^b(-u,t) - T_0^d(-u,t)] \tag{18}$$

$$K^d \frac{\partial T_0^d}{\partial y}(-u-h,t) = Q_0(t) \tag{19}$$

The first order boundary conditions are;

$$s_1(t) \frac{\partial T_0^c}{\partial y}(s_0,t) + T_1^c(s_0,t) = 0 \tag{20}$$

$$K^c[\frac{\partial T_1^c}{\partial y}(s_0,t) + s_1(t) \frac{\partial^2 T_0^c}{\partial y^2}(s_0,t)] = L_c \rho_c \frac{ds_1}{dt}(x,t) \tag{21}$$

$$K^c \frac{\partial T_1^c}{\partial y}(0,t) = K^b \frac{\partial T_1^b}{\partial y}(0,t) \tag{22}$$

$$K^b \frac{\partial T_1^b}{\partial y}(-u,t) = K^d \frac{\partial T_1^d}{\partial y}(-u,t) \tag{23}$$

$$K^c \frac{\partial T_1^c}{\partial y}(0,t) = \frac{1}{R_{sc}}[T_1^c(0,t) - T_1^b(0,t)] \tag{24}$$

$$K^b \frac{\partial T_1^b}{\partial y}(-u,t) = \frac{1}{R_{cm}}[T_1^b(-u,t) - T_1^d(-u,t)] \tag{25}$$

$$K^d \frac{\partial T_1^d}{\partial y}(-u-h,t) = Q_1(t) \tag{26}$$

4. Dimensionless Presentation

To reduce the complexness of the problem and generalize the solution, the dimensionless parameters are described as follows.

$$Y = my, \qquad S(\beta) = ms(t), \qquad H = mh, \qquad U = mu, \qquad \beta = m^2 \frac{K^c T_m}{\rho^c L^c} t, \tag{27}$$

$$\bar{T}(Y,\beta) = \frac{T(y,t)}{T_m}, \quad \bar{Q} = \frac{Q}{mK^c T_m}, \quad \bar{R}_{\mathrm{sc}} = mK^c R_{sc}, \quad \bar{R}_{\mathrm{cm}} = mK^c R_{cm} \tag{28}$$

$$\zeta_1 = \frac{K^c}{K^b}, \quad \zeta_2 = \frac{K^b}{K^d}, \quad \zeta_3 = \frac{K^c}{K^d}, \quad \epsilon_{\mathrm{c}} = \frac{K^c T_m}{\alpha^{\mathrm{c}} \rho^c L^c}, \quad \epsilon_{\mathrm{b}} = \frac{K^c T_m}{\alpha^{\mathrm{b}} \rho^c L^c}, \quad \epsilon_{\mathrm{d}} = \frac{K^c T_m}{\alpha^{\mathrm{d}} \rho^c L^c}, \tag{29}$$

The dimensionless forms of the zeroth order heat conduction equations are given below.

$$\begin{aligned} \frac{\partial^2 \bar{T}_0^c}{\partial Y^2}(Y,\beta) &= \epsilon_c \frac{\partial \bar{T}_0^c}{\partial \beta}(Y,\beta) \\ \frac{\partial^2 \bar{T}_0^b}{\partial Y^2}(Y,\beta) &= \epsilon_b \frac{\partial \bar{T}_0^b}{\partial \beta}(Y,\beta) \\ \frac{\partial^2 \bar{T}_0^d}{\partial Y^2}(Y,\beta) &= \epsilon_d \frac{\partial \bar{T}_0^d}{\partial \beta}(Y,\beta) \end{aligned} \tag{30}$$

The dimensionless zeroth-order boundary conditions used to obtain zeroth-order temperature distributions $\left(\bar{T}_0^{\,i}(x,y,t), i = c,b,d\right)$ from these equations are;

$$\bar{T}_0^c(S_0,\beta) = 1 \tag{31}$$

$$\frac{\partial \bar{T}_0^c}{\partial Y}(S_0,\beta) = \frac{dS_0(\beta)}{d\beta} \tag{32}$$

$$\frac{\partial \bar{T}_0^c}{\partial Y}(0,\beta) = \zeta_1 \frac{\partial \bar{T}_0^b}{\partial Y}(0,\beta) \tag{33}$$

$$\frac{\partial \bar{T}_0^b}{\partial Y}(-U,\beta) = \zeta_2 \frac{\partial \bar{T}_0^d}{\partial Y}(-U,\beta) \tag{34}$$

$$\frac{\partial \bar{T}_0^c}{\partial Y}(0,\beta) = \frac{1}{\bar{R}_{sc}}[\bar{T}_0^c(0,\beta) - \bar{T}_0^b(0,\beta)] \tag{35}$$

$$\frac{\partial \bar{T}_0^b}{\partial Y}(-U,\beta) = \frac{\zeta_1}{\bar{R}_{cm}}[\bar{T}_0^b(-U,\beta) - \bar{T}_0^d(-U,\beta)] \tag{36}$$

$$\frac{\partial \bar{T}_0^d}{\partial Y}(-U-H,\beta) = \zeta_3 \bar{Q}_0(\beta) \tag{37}$$

The dimensionless forms of the first order heat conduction equations are given below.

$$\frac{\partial^2 \bar{T}_1^c(Y,\beta)}{\partial Y^2} - \bar{T}_1^c(Y,\beta) = \epsilon_c \frac{\partial \bar{T}_1^c}{\partial \beta}(Y,\beta) \tag{38}$$

$$\frac{\partial^2 \bar{T}_1^b(Y,\beta)}{\partial Y^2} - \bar{T}_1^b(Y,\beta) = \epsilon_b \frac{\partial \bar{T}_1^b}{\partial \beta}(Y,\beta)$$

$$\frac{\partial^2 \bar{T}_1^c(Y,\beta)}{\partial Y^2} - \bar{T}_1^c(Y,\beta) = \epsilon_c \frac{\partial \bar{T}_1^c}{\partial \beta}(Y,\beta)$$

The dimensionless first-order boundary conditions used to obtain first-order temperature distributions $\left(\bar{T}_1^{\,i}(x,y,t), i = c,b,d\right)$ from these equations are;

$$\bar{T}_1^c(S_0,\beta)\frac{\partial \bar{T}_0^c}{\partial Y}(S_0,\beta) + \bar{T}_1^c(S_0,\beta) = 0 \tag{39}$$

$$\frac{\partial \bar{T}_1^c}{\partial Y}(S_0,\beta) + S_1(\beta)\frac{\partial^2 \bar{T}_0^c}{\partial Y^2}(S_0,\beta) = \frac{dS_1(\beta)}{d\beta} \tag{40}$$

$$\frac{\partial \bar{T}_1^c}{\partial Y}(0,\beta) = \zeta_1 \frac{\partial \bar{T}_1^b}{\partial Y}(0,\beta) \tag{41}$$

$$\frac{\partial \bar{T}_1^b}{\partial Y}(-U,\beta) = \zeta_2 \frac{\partial \bar{T}_1^d}{\partial Y}(-U,\beta) \tag{42}$$

$$\frac{\partial \bar{T}_1^c}{\partial Y}(0,\beta) = \frac{1}{\bar{R}_{sc}}[\bar{T}_1^c(0,\beta) - \bar{T}_1^b(0,\beta)] \tag{43}$$

$$\frac{\partial \bar{T}_1^b}{\partial Y}(-U,\beta) = \frac{\zeta_1}{\bar{R}_{cm}}[\bar{T}_1^b(-U,\beta) - \bar{T}_1^d(-U,\beta)] \tag{44}$$

$$\frac{\partial \bar{T}_1^d}{\partial Y}(-U-H,\beta) = \zeta_3 \bar{Q}_1(\beta) \tag{45}$$

After obtaining dimensionless equations, the numerical solution procedure for the heat transfer problem has been obtained due to a non-available closed-form solution.

5. Numerical Solution Procedure

In the heat transfer problems, the exact solutions are generally obtained just for idealized cases in which semi-finite or infinite regions are considered with simple initial/boundary conditions. Since the nonlinear behavior of this problem, the superposition principle is not applicable and all cases are evaluated separately. When the exact solution of the full Stefan problem is not calculated analytically, the numerical methods are developed to solve these problems. In this study, zero and first-order heat conduction equations (Eq. (30) and Eq. (38)) do not exist in closed form with their respective boundary conditions. For this reason, the temperature distributions and the position of the moving interface have been obtained with a numerical solution. In the current study, the Lagrange scheme, which is an explicit finite difference method, was applied to obtain the solution to the heat transfer problem during the solidification.

In the numerical solution algorithm, the shell's thickness is divided into N elements at each step. Thus, the space step width at each time step becomes $\delta = \frac{S_0(\beta)}{N}$ with the N + 1 number of nodes in the average solidified metal thickness ($0 < Y < S_0(\beta)$). In this case, the final node ($N + 1^{th}$) in the solidifying solid always corresponds to the position of the zero-order solid-liquid moving surface. Due to the increase in the average solid thickness as time progresses, the nodal points change for each new time step, and space is recalculated for

the step width. The average solidified metal thickness in the next time step depending on the time increase (τ) is calculated by the backward finite difference formulation of Eq. (32).

$$S_0^{j+1} = S_0^j + \frac{\tau}{2\delta_c}\left(3\bar{T}_{0\,N+1}^{c\,j} - 4\bar{T}_{0\,N}^{c\,j} + \bar{T}_{0\,N-1}^{c\,j}\right) \tag{46}$$

In this equation, the temperature in the moving interface ($\bar{T}_{0_{N+1}}^{j}$) is constant during the process according to Eq. (31). The temperature distributions in the solidified metal are obtained for the space variable values $Y = (i-1)\delta, (i = 1,2, \dots N+1)$ for N+1 nodes. The temperatures in the nodes in the solidified metal ($i = 2,3, \dots N$ nodes) are found for each time step with Eq. (47) which is the central finite difference formulation of the general heat conduction equation in Eq. (30a).

$$\bar{T}_{0\,i}^{c\,j+1} = \bar{T}_{0\,i}^{c\,j} + \frac{\tau}{\epsilon_c \delta_c^2}\left(\bar{T}_{0\,i+1}^{c\,j} - 2\bar{T}_{0\,i}^{c\,j} + \bar{T}_{0\,i-1}^{c\,j}\right), \quad (i = 2,3, \dots, N) \tag{47}$$

Here the subscript "i" refers to the ith node location to derive the temperature in the solidified shell while the superscript "j" is the time step counter.

In this problem, it is necessary to update with the inclusion of the convective terms in the algorithm to calculate the temperatures at the node points whose positions change depending on fixed elements number, as the thickness of the shell solidifies as time progresses.

$$\bar{T}_{0\,i}^{c\,j+1} = \bar{T}_{0\,i}^{c\,j} + (i-1)\frac{\delta_c^{j+1} - \delta_c^j}{\delta_c^j}\left(\bar{T}_{0\,i+1}^{c\,j+1} - \bar{T}_{0\,i}^{c\,j+1}\right), \quad (i = 2,3, \dots, N) \tag{48}$$

Similarly, the coating layer and mold are divided into a fixed number of elements J and M, respectively. Therefore, $J + 1$ and $M + 1$ number of nodes are formed in the coating and mold for temperature distribution derivation. As time progresses, the locations of the nodes in these layers are fixed because there is no change in coating and mold thicknesses. The temperatures for nodes ($k = 2,3, \dots, J$ and $p = 2,3, \dots, M$) in these layers are calculated by Eq. (49), which is the central finite difference formulation of Equation (30b) and Eq. (30c).

$$\begin{aligned} \bar{T}_{0\,k}^{b\,j+1} &= \bar{T}_{0\,k}^{b\,j} + \frac{\tau}{\epsilon_b \delta_b^2}\left(\bar{T}_{0\,k+1}^{b\,j} - 2\bar{T}_{0\,k}^{b\,j} + \bar{T}_{0\,k-1}^{b\,j}\right), \quad (k = 2,3, \dots, J) \\ \bar{T}_{0\,p}^{d\,j+1} &= \bar{T}_{0\,p}^{d\,j} + \frac{\tau}{\epsilon_d \delta_d^2}\left(\bar{T}_{0\,p+1}^{d\,j} - 2\bar{T}_{0\,p}^{d\,j} + \bar{T}_{0\,p-1}^{d\,j}\right), \quad (p = 2,3, \dots, M) \end{aligned} \tag{49}$$

After determining the temperatures at the nodes in the solid layers, the temperatures at the interfaces and at the mold's bottom surface are derived by using boundary conditions. For nodes, $i = 1$ and $k = J + 1$ corresponding to the solidified shell/coating interface, the temperatures are found using Eqs. (33) and (35). Similarly, the temperatures at the $k = 1$ and $p = M + 1$ nodes at the coating and mold interface are obtained using finite difference formulations of boundary conditions in Eqs. (34) and (36). Finally, the temperature of the node at the mold's lower surface ($p = 1$) is found by using Eq.(38).

The first-order solution is made using the same method as the above zeroth-order solution and the first-order temperatures at the nodes in the solid layers are obtained with $S_1(\beta)$. $S_1(\beta)$ is found by Eq. (50) which is derived through the backward finite difference formulation of Eq. (40).

$$S_1^{j+1} = S_1^j \left(1 + \frac{\tau}{\delta_c^2}\left(2\bar{T}_{0\,N+1}^{c\,j} - 5\bar{T}_{0\,N}^{c\,j} + 4\bar{T}_{0\,N-1}^{c\,j} - \bar{T}_{0\,N-2}^{c\,j}\right)\right) + \frac{\tau}{2\delta_c}\left(3\bar{T}_{1\,N+1}^{c\,j} - 4\bar{T}_{1\,N}^{c\,j} + \bar{T}_{1\,N-1}^{c\,j}\right) \tag{50}$$

Similar to the zeroth degree solution, the first order node temperatures are calculated using the heat conduction equations in Eq. (38) and the first-order boundary conditions in Eq. (39) and Eqs. (41) - (45).

Another important factor is the adjustment of the time increment variable (τ) in the algorithm. The discretization of both time and dimensional variables is of great importance for the reliability of the results obtained by the numerical solution. For this reason, when choosing the value of τ, attention should be paid to the acceptance of numerical convergence, to maintain stability and to provide calculation efficiency. The maximum time step for stability is proportional to $\epsilon_c\delta_c^2$. Therefore, the stability condition imposes a restriction on τ when good spatial accuracy is required, which usually requires very small δ values. In this case, the numerical stability for this model occurs when the conditions in Eq. (51) are provided.

$$\frac{\tau}{\epsilon_c\delta_c^2} < 0.5, \quad \frac{\tau}{\epsilon_b\delta_b^2} < 0.5, \quad \frac{\tau}{\epsilon_d\delta_d^2} < 0.5 \tag{51}$$

When solidification begins, $S_0(\beta)$ and δ are of very small values. Hence, a very small time step is needed to fulfill the requirement in Eq.(51a). But choosing the time step so small causes the algorithm to be very slow. In the continuation of solidification, the time step is allowed to increase without loss of stability due to the increase in $S_0(\beta)$ and δ. However, the conditions in Eq.(51b) and Eq.(51c) significantly limit this increase in T due to the constant δ_b and δ_d during solidification. Therefore, it is necessary to use a very small initial δ value during the solidification process to keep both space and time steps under conditions and obtain a reliable result.

Also, the nodes must not overlap for the algorithm used for the numerical solution. For this reason, solidification is not desired to start at $S_0(\beta) = 0$. To overcome this problem, an appropriate initial condition must be created and the solution of the limiting problem under certain assumptions is used for this purpose. In the early stages, the limited solution is of acceptable accuracy. Therefore, the numerical solution of the considered problem, in which the material thermal diffusivities are included, was started by using this limiting solution with a very small finite $S_0(\beta)$. The solution to this limiting problem is presented by Demir and Yigit [38] and the expressions used as the initial condition for the numerical solution are given in the Appendix.

6. Results and Discussion

In this study, the numerical solution of the heat transfer problem, which is one of the sub-parts of the thermoelasticity problem that occurs during solidification, was carried out, and especially the roles of the coating layer on the thermoelastic instability were dealt with. The theoretical model developed by Demir and Yigit [38], which examines the heat transfer problem at the early stages of the process, was used as the initial condition in the solution of the full heat transfer problem, in which the thermal capacities of the solidifying metal, coating layer and mold materials are not considered zero (the thermal diffusivities of the materials are assumed to have finite values).

At the beginning of the analysis, obtained numerical results are compared with the previous results in Yigit [33] in which the heat transfer problem during the solidification

of pure metal on planar mold without a coating layer. Therefore, the coating layer's effects on the process is neglected for proving the correctness of the solution by assuming $U + H = 10$, $\bar{R}_{\mathrm{cm}} \ll 1$, $\zeta_2 = 1, \epsilon_2 = \epsilon_3 = 10$, $\zeta_1 = \zeta_3 = 2$, $\bar{R}_{\mathrm{sc}} = \bar{R}_0$ when $\bar{R}_0 = 0.3$, $\zeta_1 = 2$ for approaching the model in Yigit [33].

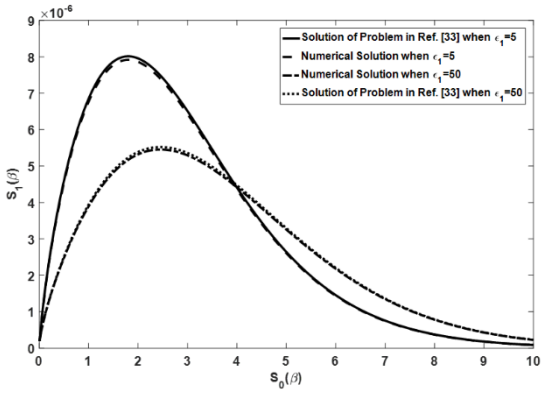

Fig. 2 The comparison between the numerical solution and the limiting solution in Yigit [33] when $\epsilon_1 = 5$ and $\epsilon_1 = 50$ ($U + H = 10, \bar{R}_{\mathrm{cm}} \ll 1$, $\zeta_2 = 1, \epsilon_2 = \epsilon_3 = 10$, $\zeta_1 = \zeta_3 = 2$, $\bar{R}_{\mathrm{sc}} = \bar{R}_0 = 0.3$)

The mold and coating are assumed to make of the same material and $\bar{R}_{cm}$ is considered very small. Thus, we converge to the solution given in Fig. 4 in Ref [33] where $H = 10, \zeta = 2, \bar{R}_0 = 0.3, \epsilon_1 = 5$ and $\epsilon_2 = 10$. The comparison results are given in Fig. 2 for different values of ϵ_1. Fig. 2 shows the variation of $S_1(\beta)$ as a function of $S_0(\beta)$ for the numerical solution and Yigit's problem solution when $\epsilon_1 = 5$ and $\epsilon_1 = 50$. The results of the present model go to limiting solutions due to Yigit [33] and it is indicated that these results are important in terms of proving the accuracy and reliability of the developed finite-difference algorithm and the numerical solution procedure. Thus, it can be said that the results examining the effects on the problem of heat transfer during solidification in which the coating layer is included in the later stages are reliable and reflect the actual process within certain assumptions. After that, the influences of the coating's thickness on the thermoelastic stability during the solidification are examined.

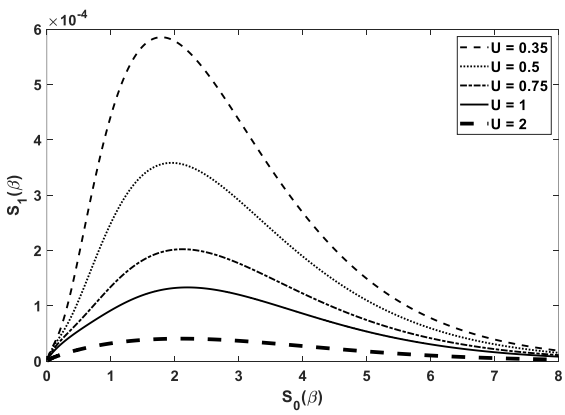

Fig. 3 The variation of $S_1(\beta)$ as a function of $S_0(\beta)$, at selected values of U when $H = 5, \zeta_1 = \zeta_2 = 0.5, \epsilon_1 = \epsilon_2 = \epsilon_3 = 10$ and $\bar{R}_{sc} = \bar{R}_{cm} = 0.3$

Fig. 3 shows the variation of $S_1(\beta)$ for different coating thickness. Other parameters are assumed $H = 5, \zeta_1 = \zeta_2 = 0.5, \epsilon_1 = \epsilon_2 = \epsilon_3 = 10$ and $\bar{R}_{sc} = \bar{R}_{cm} = 0.3$. The results indicate that the coating layer controls the heat transfer during solidification and it leads to stabilizing effect. In other words, the thicker coating layer should be chosen as much as possible to achieve more stable growth and better quality final casting. It should also be mentioned here that increasing the coating thickness for all solidification parameter combinations creates a stability-enhancing effect. These effects of the coating layer are shown in the following figures in detail. Likewise, it is seen that the thickness of the mold has a similar effect and it is concluded that this supports the fact that increasing the layer thickness directly enables the heat transfer rate to be controlled.

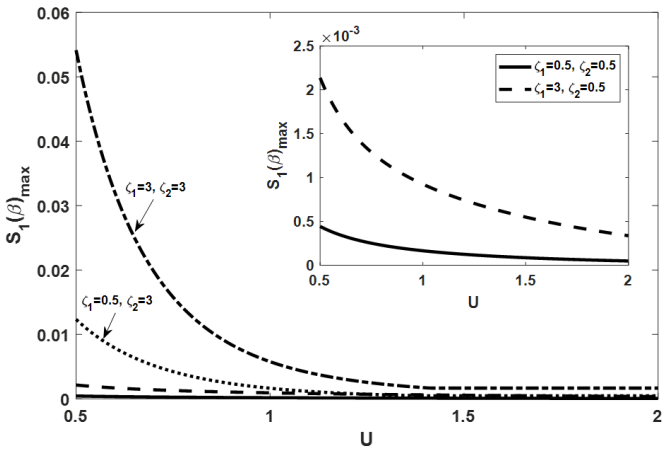

Fig. 4 The variation of $S_1(\beta)_{max}$ as a function of U for four combinations of ζ_1 and ζ_2 ($H = 5, \epsilon_1 = 2, \epsilon_2 = \epsilon_3 = 5, \bar{R}_{\mathrm{sc}} = \bar{R}_{\mathrm{cm}} = 0.3$)

Then, the effect of the thickness of the coating layer is focused depending on the other important process parameters such as conductivity ratios and thermal capacities. Fig. 4 shows the variation of $S_1(\beta)_{max}$ as a function of coating thickness, U, for different values of thermal conductivity ratios between materials of the shell, mold and its coating when $\epsilon_1 = 2, \epsilon_2 = \epsilon_3 = 5, \bar{R}_{\mathrm{sc}} = \bar{R}_{\mathrm{cm}} = 0.3$. $S_1(\beta)_{max}$ denotes the maximum amplitude of the perturbed undulation on the mean shell thickness. The aim here is to establish the relationship between the choice of mold, coating, and casting materials and the coating thickness and to create clues for the most efficient casting. The results show that the thermal conductivity ratios have an important effect on growth instability and the sensitivity to coating thickness. It is indicated that the coating's thickness has stabilizing impact for all combinations of ζ_1 *and* ζ_2. However, it is seen that this effect varies considerably according to the values of these parameters. The ζ_1 and ζ_2 values selected in this figure represent various orders of material thermal conductivities relative to each other. $\zeta_1 = 0.5$ - $\zeta_2 = 0.5$, $\zeta_1 = 3$ - $\zeta_2 = 0.5$, $\zeta_1 = 0.5$ - $\zeta_2 = 3$ and $\zeta_1 = 3$ - $\zeta_2 = 3$ represent the cases in which the values of the thermal conductivities are ranked as $K^d > K^b > K^c$, $K^c > K^d > K^b$, $K^b > K^c > K^d$ and $K^c > K^b > K^d$, respectively. The results show that $\zeta_1 =$ 0.5 - $\zeta_2 = 0.5$ case leads to more uniform growth than the other cases and the most unstable growth occurs when ζ_1 and ζ_2 are equal to 3. In other words, $K^c > K^b > K^d$ state causes the most unstable growth, while $K^d > K^b > K^c$ the condition causes the most stable growth. Also, much lower amplitude perturbations occur when $K^d > K^b > K^c$ and $K^c > K^d > K^b$. This means that if the coating material is chosen from a material whose thermal conductivity is smaller than that of the mold material, the growth instability is minimized to obtain the best quality casting piece, regardless of the shell's thermal

conductivity. Besides, the smaller thermal conductivity of the casting material compared to that of both the mold and the coating material ensures the most efficient solidification. The most unstable growth occurs when the mold's thermal conductivity is the smallest. In those cases, where the shell's conductivity is greater than that of the mold, the coating's thermal conductivity should be chosen higher than that of the material to be cast for quality solidification.

Furthermore, it can be seen from this figure that the sensitivity to the change of coating thickness varies according to the thermal conductivities. For $\zeta_1 = 3$ - $\zeta_2 = 3$, it is seen that the change in x according to the change of the coating thickness of the process is the most and the sensitivity to the coating thickness is the most in this case. Following this case, coating thickness sensitivity for $\zeta_1 = 0.5$ - $\zeta_2 = 3$ is also higher than in other cases. Thus, it can be said that in the case where the mold's thermal conductivity is the smallest, the sensitivity of the solidification process to the thickness increases. Relatively, for cases where $\zeta_1 = 0.5$ - $\zeta_2 = 0.5$, $\zeta_1 = 3$ - $\zeta_2 = 0.5$, it is seen that the sensitivity to the coating thickness decreases. Therefore, in cases where the sensitivity to coating thickness is to be lowered, the mold's thermal conductivity should be chosen greater than that of the coating regardless of the thermal conductivity of the metal to be solidified. However, it should be studied where the coating's thermal conductivity is greater than that of the other solid layers to minimize the sensitivity to the coating thickness. According to the results, the thermal conductivity ratios play an important role on the growth instability. Fig. 5 shows the variation of $S_1(\beta)_{max}$ depending on the thermal conductivity ratios (ζ_1 and ζ_2) when $U = 0.5, H = 5, \epsilon_1 = \epsilon_2 = \epsilon_3 = 5$ and $\bar{R}_{\mathrm{sc}} = \bar{R}_{\mathrm{cm}} = 0.3$. The curves in the figure were obtained by keeping one of the thermal conductivity ratios constant and changing the other so that the effects of the change of thermal conductivity of the materials relative to each other on the growth instability were observed.

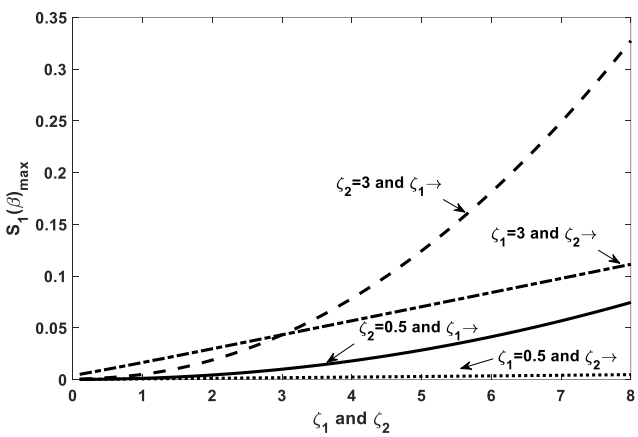

Fig. 5 The variation of $S_1(\beta)_{max}$ as a function of ζ_1 and ζ_2 for the case where $U = 0.5, H = 5, \epsilon_1 = \epsilon_2 = \epsilon_3 = 5$ and $\bar{R}_{\mathrm{sc}} = \bar{R}_{\mathrm{cm}} = 0.3$

The results show that the increases in both ζ_1 and ζ_2 increase the amplitude of the perturbations at the moving interface and have negative effects on the growth instability. It can be also seen that it is seen that the change of ζ_2 varies the amplitude of the perturbations least when $\zeta_1 = 0.5$. In this case, it appears that the solidification process has less sensitivity to ζ_2, and changing the value of K^d for $K^b > K^c$ has less effect on growth instability. It is observed that an increase in ζ_1 leads to increase in the sensitivity of the process to change of ζ_2. This means that the variation of the mold's thermal conductivity

affects the thermoelastic stability much more when the shell's conductivity is higher than the coating's conductivity. Similarly, for $\zeta_2 = 0.5$ and $\zeta_2 = 3$, the effect of changing ζ_1 also appeared to increase instability. Again, according to the value of ζ_2, the sensitivity of the process to ζ_1 varies. It is seen that the sensitivity to ζ_1 increases when ζ_2 is greater than 1 than the case where ζ_2 is less than 1. This means that both growth instability and sensitivity to the coating's and shell's conductivities are increased when the coating thermal conductivity is greater than that of the mold, compared to the case where it is smaller than the mold's conductivity.

On the other hand, the specific heats of the materials vary the coating layer's effects on the process. Fig. 6 shows the variation of $S_1(\beta)_{max}$ as a function of coating thickness for the different combinations of the specific heat values of the solid layer's materials when $H = 5, \zeta_1 = \zeta_2 = 2$ and $\bar{R}_{\mathrm{sc}} = \bar{R}_{\mathrm{cm}} = 0.3$. All specific heat values are taken as 3, 10 and 50 and compared with the case where all specific heat values are equal to 10. As mentioned earlier, the stability-enhancing effect of the coating thickness is seen for all considered specific heats combinations and it is seen that the change of the specific heat values changes the sensitivity to the coating thickness.

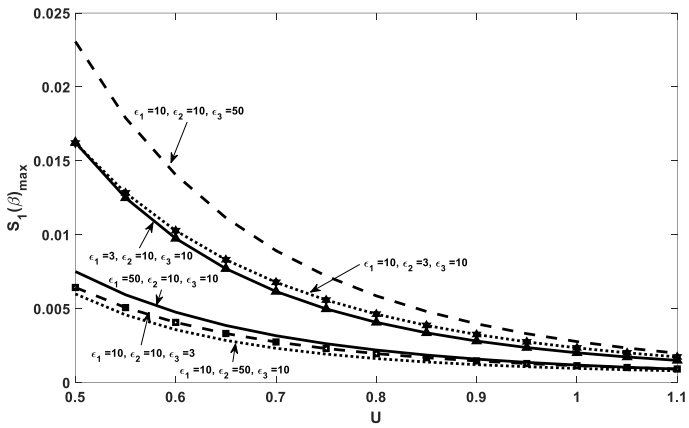

Fig. 6 The variation of $S_1(\beta)_{max}$ depending on U for the different values of ϵ_1, ϵ_2 and ϵ_3 ($H = 5, \zeta_1 = \zeta_2 = 2$ and $\bar{R}_{\mathrm{sc}} = \bar{R}_{\mathrm{cm}} = 0.3$)

The results show that the increase in ϵ_3 appears to cause larger amplitude perturbation for a given coating thickness, while the increases in ϵ_1 and ϵ_2 cause lower amplitude perturbations. Therefore, the decrease in $S_1(\beta)_{max}$ due to the increase in coating thickness occurs when the value of ϵ_3 is large. Thus, it can be said that increasing the specific heat of the mold material increases the sensitivity to coating thickness. Considering the stability-enhancing effects of ϵ_1 and ϵ_2, it is seen that the sensitivity to coating thickness is high when ϵ_1 and ϵ_2 are small, It is also observed that the sensitivity to the coating thickness is reduced for large values of ϵ_1 and ϵ_2 and for small values of ϵ_3. Physically, this result raises the requirement that certain temperatures of the solidified metal and the material of the coating layer should be low or the mold should be selected from the material with a certain temperature in order to reduce the dependence of the solidification process on the coating thickness. It can be also noted that the effects of the specific heat of the materials of the solid layers on the growth instability are opposite and these effects of the specific heats have been examined in Fig. 7.

The variation of $S_1(\beta)_{max}$ depending on the specific heat values of materials ($\epsilon_1, \epsilon_2, \epsilon_3$) is shown in Fig. 7 when $U = 0.5, H = 5, \zeta_1 = 0.5$ and $\zeta_2 = 3$. The specific heats change from

0.1 to 20 for each curve in the figure and the curves are drawn for the cases where each specific heat changes, whereas the other two specific heats are equal to 10. The results indicate that the specific heat of each solid layer has different effects on the unstable shell growth and the sensitivity of the solidification process to these specific heat variations is also different. It is seen that the specific heats of solidified shell and coating materials have stabilizing effects on the growth stability during the solidification. This means that they should be selected higher specific heats (lower thermal diffusivities) for more uniform growth and higher quality final cast. However, the higher specific heat of mold material causes an increase in $S_1(\beta)_{max}$, and hence, it reduces growth stability. As can be seen, while ϵ_1 and ϵ_2 increase stability, ϵ_3 has an increasing effect on unstable shell growth for the considered case. When analyzes are made for all cases, it is seen that the specific heats of the materials have a similar effect on the process. Therefore, it can be said that the effects of the specific heat of the solidified metal and the coating layer (ϵ_1 and ϵ_2) and the mold's specific (ϵ_3) on the perturbation growth neutralize each other. It can also be stated that the sensitivity of the growth instability to ϵ_2 variation during the solidification process is quite low, but the sensitivities to ϵ_1 and ϵ_3 variations are high.

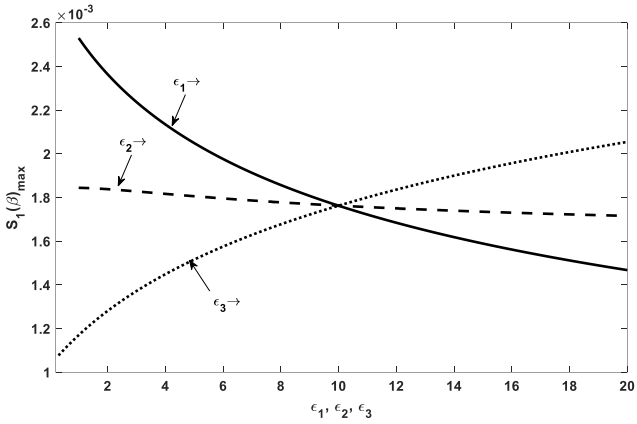

Fig. 7 The variation of $S_1(\beta)_{max}$ as a function of ϵ_1, ϵ_2 and ϵ_3 for the case where $U = 0.5, H = 5, \zeta_1 = 0.5, \zeta_2 = 3$ and $\bar{R}_{\mathrm{sc}} = \bar{R}_{\mathrm{cm}} = 0.3$

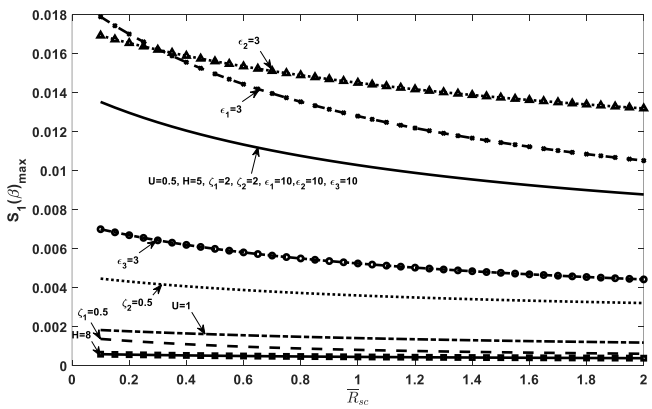

Fig. 8 The variation of $S_1(\beta)_{max}$ as a function of $\bar{R}_{\mathrm{sc}}$ for the different values of system parameters

The effects of the thermal contact resistances ($\bar{R}_{\mathrm{sc}}, \bar{R}_{\mathrm{cm}}$) are analyzed in Fig. 8 and Fig. 9, respectively. These figures show the variation of $S_1(\beta)_{max}$ as a function of thermal contact resistances. They are changed from 0.1 to 2 because the aforementioned effects were found to be unchanged for the values greater than 2. Additionally, it was observed how the effects of thermal resistances on growth instability changed for different values of other system parameters. Firstly, the variation of $S_1(\beta)_{max}$ is observed as a function of $\bar{R}_{\mathrm{sc}}$ in Fig. 8. The straight line curve represents the case in which the other system parameters are assumed to be equal as $U = 0.5, H = 5, \zeta_1 = \zeta_2 = 2, \bar{R}_{\mathrm{cm}} = 0.3$ and $\epsilon_1 = \epsilon_2 = \epsilon_3 = 10$.

The result indicates that an increase in $\bar{R}_{\mathrm{sc}}$ causes a decrease in the maximum amplitude of perturbation at the freezing front. This indicates that the thermal resistance at the shell/coating interface should be increased for more stable growth and better quality final cast. The other cases in the figure show the cases that occur by changing only one of the values of the system parameters given for the situation specified with the straight-line curve. It also appears that the same stabilizing effect applies to all cases in the figure. Although the variation of system parameters generally does not change the stability-enhancing effect of $\bar{R}_{\mathrm{sc}}$, it has been observed that the sensitivity of the process to $\bar{R}_{\mathrm{sc}}$ varies with the values of the system parameters. It is seen from the results that the decrease in ζ_1 and ζ_2 has decreased sensitivity to $\bar{R}_{\mathrm{sc}}$. Similarly, it was found that the increase in U and H decrease this sensitivity. Then, if the sensitivity to thermal contact resistance at this interface is to be reduced, it is necessary to increase the thickness of the coating and mold, to choose the thermal conductivity of the casting material smaller than the coating material, and to choose the coating material from the material with thermal conductivity less than the mold's conductivity. When the specific heats of materials are examined, it is seen that the sensitivity to $\bar{R}_{\mathrm{sc}}$ increases with the decrease of ϵ_1 but does not change significantly with the decrease of ϵ_2 and ϵ_3. From this situation, it is seen that the sensitivity to thermal contact resistance between this layer and the coating layer can be adjusted by changing the shell's specific heat.

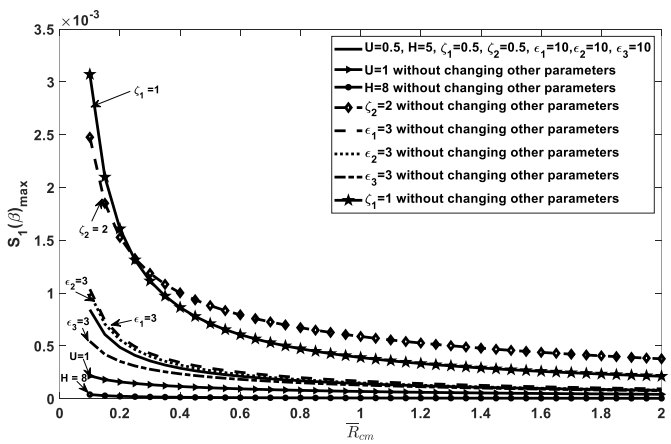

Fig. 9 The variation of $S_1(\beta)_{max}$ with respect to $\bar{R}_{\mathrm{cm}}$ for the different values of system parameters

The effects of $\bar{R}_{\mathrm{cm}}$ are investigated in Fig. 9 in which the variation of $S_1(\beta)_{max}$ as a function of $\bar{R}_{\mathrm{cm}}$ for different values of other system parameters. Similar to Fig. 8, the straight-line curve is the main curve in which the system parameters are assumed to be equal as $U = 0.5, H = 5, \zeta_1 = \zeta_2 = 0.5, \bar{R}_{\mathrm{sc}} = 0.3$ and $\epsilon_1 = \epsilon_2 = \epsilon_3 = 10$ and other cases represent the cases in which only one system parameter is changed. The results show that $S_1(\beta)_{max}$

decreases when $\bar{R}_{\mathrm{cm}}$ is increased. This means that both $\bar{R}_{\mathrm{sc}}$ and $\bar{R}_{\mathrm{cm}}$ have stabilizing effects on the shell's growth. Physically, these thermal contact resistances should be increased for better quality final cast. It is also seen that the sensitivity of the process to $\bar{R}_{\mathrm{cm}}$ is greater than the sensitivity to $\bar{R}_{\mathrm{sc}}$. Similar to the results in Fig. 9, the sensitivity of $\bar{R}_{\mathrm{cm}}$ decreases when ζ_1 and ζ_2 decrease. Moreover, increases in U and H also decrease this sensitivity. It is also noteworthy that decreases in ϵ_1 and ϵ_2 cause an increase in the sensitivity of $\bar{R}_{\mathrm{cm}}$ but on the contrary, the decrease in ϵ_3 decreases the sensitivity. Therefore, it can be said that the shell's and coating's specific heats should be selected higher and the mold's specific heat should be selected lower for reducing dependence to $\bar{R}_{\mathrm{cm}}$. These results mean that thicker coating and mold lead to a decrease in the effect of $\bar{R}_{\mathrm{cm}}$ on the proses and the coating's thermal conductivity should be selected higher than the shell's conductivity for reducing the dependence on changes of $\bar{R}_{\mathrm{cm}}$. Also, this dependence of the process can be reduced by the selection of the mold's thermal conductivity greater than the coating's conductivity.

7. Conclusion

A theoretical model is developed to study the effects of the coating layer on the growth instability mechanism during the solidification of pure metal on a coated mold of finite thickness. The phase change heat transfer problem, which is one of the two main sub-problems of thermoelastic instability during solidification, is considered, modeled, and solved numerically in this study. This study extends previous studies by taking into account the combined effects of coating layer properties and thermal capacitances of solid layers. The spatial dimension of the modeled heat transfer problem was reduced from two to one dimensional with the linear perturbation method. The finite acceptance of thermal diffusivities provides that the obtained full solidification model has to be solved numerically due to the nonlinear behavior of phase change problems. Therefore, the governing equations are discretized by the Lagrangian finite difference scheme for numerical solution. In this numerical solution, a limiting solution is used as initial conditions, and this limiting solution is obtained analytically in [38] by assuming the thermal diffusivities of the materials are infinite. The key question is how the properties of the coating layer are selected according to the other parameters.

The results show that an increase in the coating's thickness causes a positive effect on the thermoelastic instability and the thicker coating layer should be chosen as much as possible to achieve more stable growth and better quality final casting. Also, a thicker coating layer creates a stability-enhancing effect for all solidification parameter combinations. But, it is observed that the stabilizing effect of this thickness varies considerably according to the values of other parameters.

The sensitivity to coating thickness is to be lowered when the mold's thermal conductivity should be chosen greater than that of the coating material regardless of the thermal conductivity of the metal to be solidified. However, it should be worked in the cases in which the coating's thermal conductivity is greater than that of the other solid layers in order to minimize the coating thickness's dependence of the process. When the effects of the specific heats on this coating thickness dependence of the process are investigated, it is also observed that the sensitivity to the coating thickness is reduced for large values of ϵ_1 and ϵ_2 and for small values of ϵ_3. On the other hand, it is also stated that the increases in both ζ_1 and ζ_2 increase $S_1(\beta)$ and have negative effects on the thermoelastic stability. Moreover, ϵ_3 shows an increasing effect on growth instability while ϵ_1 and ϵ_2 increase the stability for all cases and this means that the effects of the shell's and coating's specific heats and the mold's specific heat neutralize each other. Finally, the thermal contact resistances have stabilizing effects for all cases but the sensitivities of the process to these resistances vary according to other parameters.

The solution of this study can be used in uncoupled and coupled problems in which the thermos-mechanical problem is investigated for analyzing the full solidification process.

Appendix

In this section, the limiting solution of the heat transfer problem during the pure metal solidification process on a coated planar mold is given. The limiting solution is obtained when the thermal diffusivities of the materials are assumed to be infinite ($\epsilon_c \to 0, \epsilon_b \to 0$ *and* $\epsilon_d \to 0$). An analytical solution for the temperature fields in the solid layer and the position of the moving interface are derived for the limiting case in which the effects of the materials' thermal capacity are negligible. This model is valid for only the early stages and in the full problem, in which thermal diffusivities are finite,-this limiting solution is used as initial conditions. The limiting solution is obtained in Demir and Yigit [38] and the readers refer to this study for more details. In summary, the expressions that are important for this study and give the average shell thickness and node temperatures in solid layers for a very small time interval are given below.

Zeroth-order temperature fields are;

$$\begin{aligned}
&\bar{T}_0^c(Y,\beta) = 1 + \bar{Q}_0(\beta)(\mathrm{Y} - S_0(\beta)) \\
&\bar{T}_0^b(Y,\beta) = 1 + \bar{Q}_0(\beta)(\zeta_1\mathrm{Y} - S_0(\beta) - \bar{R}_{\mathrm{sc}}) \\
&\bar{T}_0^d(Y,\beta) = 1 + \bar{Q}_0(\beta)(\zeta_3\mathrm{Y} - \zeta_1\mathrm{U} - S_0(\beta) + \zeta_3\mathrm{U} - \bar{R}_{\mathrm{sc}} - \bar{R}_{\mathrm{cm}})
\end{aligned} \tag{A.1}$$

The mean shell thickness is;

$$S_0(\beta) = \bar{Q}_0(\beta)\beta \tag{A.2}$$

First-order temperature fields are;

$$\begin{aligned}
&\bar{T}_1^c(Y,\beta) = C_1(\beta)\sinh(Y) + C_2(\beta)\cosh(Y) \\
&\bar{T}_1^b(Y,\beta) = C_3(\beta)\sinh(Y) + C_4(\beta)\cosh(Y) \\
&\bar{T}_1^d(Y,\beta) = C_5(\beta)\sinh(Y) + C_6(\beta)\cosh(Y)
\end{aligned} \tag{A.3}$$

The perturbed undulation on the mean shell thickness is given in Eq. (A4) as follows.

$$\mathrm{S}_1\big(S_0(\beta)\big) = \frac{C_7\, S_0(\beta)}{C_8\cosh\big(S_0(\beta)\big) + C_9\sinh\big(S_0(\beta)\big)} \tag{A.4}$$

The coefficients are;

$$\begin{aligned}
&\bar{C}_1 = A_{32} + A_{33}S_1(\beta), \quad \bar{C}_2 = A_{34} + A_{35}S_1(\beta), \quad \bar{C}_3 = A_{37} + A_{38}S_1(\beta) \\
&\bar{C}_4 = A_{39} + A_{40}S_1(\beta) \quad \bar{C}_5 = A_{44} + A_{45}S_1(\beta), \quad \bar{C}_6 = A_{42} + A_{43}S_1(\beta) \\
&\bar{C}_7 = A_{29}, \quad \bar{C}_8 = A_{27}, \quad \bar{C}_9 = A_{28}
\end{aligned} \tag{A.5}$$

The coefficients $A_{1.....45}$ are given in the Appendix part of Demir and Yigit [38] paper.

References

[1] Hanao M, Kawamoto M, Yamanaka, A. Growth of solidified shell just below the meniscus in continuous casting mold. ISIJ International, 2009; 49(3): 365-374. https://doi.org/10.2355/isijinternational.49.365

[2] Yigit F, Barber J. Effect of Stefan number on thermoelastic instabilities in unidirectional solidification. International Journal of Mechanical Sciences, 1994; 36(8): 707-723. https://doi.org/10.1016/0020-7403(94)90087-6
[3] Konishi J, Militzer M, Samarasekera IV, Brimacombe JK. Modeling the formation of longitudinal facial cracks during continuous casting of hypoperitectic steel. Metallurgical and Materials Transactions B, 2002; 33(3): 413-423. https://doi.org/10.1007/s11663-002-0053-y
[4] Demir MH. (2016) Thermoelastic stability analysis of solidification of pure metals on a coated planar mold of finite thickness: effects of the coating layer. Ph. D. Dissertation, Yıldız Technical University, Istanbul. https://doi.org/10.1007/s11663-016-0876-6
[5] Stefan J. Uber die Theorie Der Eisbildung, insbesondere Uber die Eisbildung im Polarmeere. Annalen der Physik, 1891; 278(2): 269-286. https://doi.org/10.1002/andp.18912780206
[6] Evans GW. A note on the existence of a solution to a problem of Stefan. Quarterly of Applied Mathematics, 1951; 9(2): 185-193. https://doi.org/10.1090/qam/43330
[7] Douglas J. A uniqueness theorem for the solution of a Stefan problem. Proceedings of the American Mathematical Society, 1957; 8(2): 402-402. https://doi.org/10.1090/S0002-9939-1957-0092086-6
[8] Crank J. Free and moving boundary problems, Oxford University Press, UK, 1987.
[9] Hill JM. One-dimensional Stefan problems: An introduction, Longman Sc & Tech., USA, 1987.
[10] Barry SI, Caunce J. Exact and numerical solutions to a Stefan problem with two moving boundaries. Applied Mathematical Modelling, 2008; 32(1): 83-98. https://doi.org/10.1016/j.apm.2006.11.004
[11] Song T, Upreti K, Subbarayan G. A sharp interface isogeometric solution to the Stefan problem. Computer Methods in Applied Mechanics and Engineering, 2015; 284: 556-582. https://doi.org/10.1016/j.cma.2014.10.013
[12] Reutskiy S. A meshless method for one-dimensional Stefan problems. Applied Mathematics and Computation, 2011; 217(23): 9689-9701. https://doi.org/10.1016/j.amc.2011.04.053
[13] Juric D, Tryggvason G. A front-tracking method for dendritic solidification. Journal of Computational Physics, 1996; 123(1): 127-148. https://doi.org/10.1006/jcph.1996.0011
[14] Murray WD, Landis F. Numerical and machine solutions of transient heat-conduction problems involving melting or freezing: Part I-Method of analysis and sample solutions. Journal of Heat Transfer, 1959; 81(2): 106-112. https://doi.org/10.1115/1.4008149
[15] Segal G, Vuik K, Vermolen F. A conserving Discretization for the free boundary in a two-dimensional Stefan problem. Journal of Computational Physics, 1998; 141(1): 1-21. https://doi.org/10.1006/jcph.1998.5900
[16] Kutluay S, Bahadir A, Özdeş A. The numerical solution of one-phase classical Stefan problem. Journal of Computational and Applied Mathematics, 1997; 81(1): 135-144. https://doi.org/10.1016/S0377-0427(97)00034-4
[17] Caldwell J, Savovic' S, Kwan Y. Nodal integral and finite difference solution of one-dimensional Stefan problem. Journal of Heat Transfer, 2003; 125(3): 523-527. https://doi.org/10.1115/1.1565091
[18] Caldwell J, Kwan Y. Numerical methods for one-dimensional Stefan problems. Communications in Numerical Methods in Engineering, 2004; 20: 535-545. https://doi.org/10.1002/cnm.691
[19] Chen S, Merriman B, Osher S, Smereka P. A simple level set method for solving Stefan problems. Journal of Computational Physics, 1997; 135(1): 8-29. https://doi.org/10.1006/jcph.1997.5721

[20] Font F. A one-phase Stefan problem with size-dependent thermal conductivity. Applied Mathematical Modelling, 2018; 63: 172-178. https://doi.org/10.1016/j.apm.2018.06.052
[21] Mackenzie J, Robertson M. A moving mesh method for the solution of the one-dimensional phase-field equations. Journal of Computational Physics, 2002; 181(2): 526-544. https://doi.org/10.1006/jcph.2002.7140
[22] Sun Y, Beckermann C. Sharp interface tracking using the phase-field equation. Journal of Computational Physics, 2007; 220(2): 626-653. https://doi.org/10.1016/j.jcp.2006.05.025
[23] Vynnycky M, Mitchell S. On the numerical solution of a Stefan problem with finite extinction time. Journal of Computational and Applied Mathematics, 2015; 276: 98-109. https://doi.org/10.1016/j.cam.2014.08.023
[24] Myers T, Mitchell S. Application of the combined integral method to Stefan problems. Applied Mathematical Modelling, 2011; 35(9): 4281-4294. https://doi.org/10.1016/j.apm.2011.02.049
[25] Zabaras N, Mukherjee S. An analysis of solidification problem by the boundary element method. International Journal for Numerical Methods in Engineering, 1987; 24: 1879-1900. https://doi.org/10.1002/nme.1620241006
[26] Dursunkaya Z, Nair S. Solidification of a finite medium subject to a periodic variation of boundary temperature. Journal of Applied Mechanics, 2003; 70(5): 633-637. https://doi.org/10.1115/1.1604836
[27] Skrzypczak T, Węgrzyn-Skrzypczak E. Mathematical and numerical model of solidification process of pure metals. International Journal of Heat and Mass Transfer, 2012; 55(15-16): 4276-4284. https://doi.org/10.1016/j.ijheatmasstransfer.2012.03.070
[28] Caldwell J, Kwan Y. On the perturbation method for the Stefan problem with time-dependent boundary conditions. International Journal of Heat and Mass Transfer, 2003; 46(8): 1497-1501. https://doi.org/10.1016/S0017-9310(02)00415-5
[29] Yu Z, Fan L, Hu Y, Cen K. Perturbation solution to heat conduction in melting or solidification with heat generation. Heat and Mass Transfer, 2010; 46(4): 479-483. https://doi.org/10.1007/s00231-010-0596-4
[30] Yigit F. A simplified analytical solution of a two-dimensional Stefan problem with a periodic boundary condition. International Review of Mechanical Engineering, 2007; 1: 703-714.
[31] Yigit F. Perturbation solution for solidification of pure metals on a sinusoidal mold surface. International Journal of Heat and Mass Transfer, 2007; 50(13-14): 2624-2633. https://doi.org/10.1016/j.ijheatmasstransfer.2006.11.023
[32] Yigit F. Approximate analytical and numerical solutions for a two-dimensional Stefan problem. Applied Mathematics and Computation, 2008; 202(2): 857-869. https://doi.org/10.1016/j.amc.2008.03.033
[33] Yigit F. Sinusoidal perturbation solution for solidification of pure materials on a planar mold of finite thickness. International Journal of Thermal Sciences, 2008; 47: 25-34. https://doi.org/10.1016/j.ijthermalsci.2007.01.016
[34] Sanz A. Tribological behavior of coatings for continuous casting of steel. Surface and Coating Technology, 2001; 146-147: 55-64. https://doi.org/10.1016/S0257-8972(01)01475-X
[35] Jafari H, Idris MH, Ourdjini A, Karimian M, Payganeh G. Influence of gating system, sand grain size, and mould coating on microstructure and mechanical properties of thin-wall ductile iron. Journal of Iron and Steel Research International, 2010; 17(12): 38-45. https://doi.org/10.1016/S1006-706X(10)60195-1
[36] Karimian M, Ourdjini A, Hasbullah Idris M, Jafari H. Effect of pattern coating thickness on characteristics of lost foam Al-SI-Cu alloy casting. Transactions of Nonferrous Metals

Society of China, 2012; 22(9): 2092-2097. https://doi.org/10.1016/S1003-6326(11)61433-7

[37] Hamasaiid A, Dargusch M, Davidson C, Tovar S, Loulou T, Rezaï-Aria F, Dour G. Effect of mold coating materials and thickness on heat transfer in permanent mold casting of aluminum alloys. Metallurgical and Materials Transactions A, 2007; 38(6): 1303-1316. https://doi.org/10.1007/s11661-007-9145-2

[38] Demir MH, Yigit F. Uncoupled modeling of the effects of coating layer on the growth instability in pure metal solidification. International Journal of Metalcasting, 2021; 15, 326-337. https://doi.org/10.1007/s40962-020-00470-x

[39] Demir MH, Yigit F. Effect of coating material on the growth instability in solidification of pure metals on a coated planar mold of finite thickness. International Journal of Solids and Structures, 2016; 99: 12-27. https://doi.org/10.1016/j.ijsolstr.2016.08.010

[40] Demir MH, Yigit F. Thermoelastic stability analysis of solidification of pure metals on a coated planar mold of finite thickness, Metallurgical and Materials Transactions B, 2017; 48 (2), 966-982. https://doi.org/10.1007/s11663-016-0876-6

[41] Demir MH, Yigit F. A theoretical heat transfer model for unidirectional solidification of pure metals on a coated sinusoidal mold with constant boundary temperature. Arabian Journal for Science and Engineering, 2019; 44(6): 5825-5837. https://doi.org/10.1007/s13369-019-03736-7